Mutual Coupling Reduction in UWB MIMO Antenna Using T-Shaped Stub

Kondapalli Venu Gopal* and Yarravarapu Srinivasa Rao

Abstract—A $26 \times 25\,\text{mm}^2$ arbitrary-shaped antenna is constructed in this article, and it was expanded to 2×2 Multiple Input Multiple Output (MIMO) antenna. It has a range of 3.1 to $8.2\,\text{GHz}$. A T-shaped stub is employed in this instance to reduce the mutual coupling between the two ports. The effectiveness of the MIMO aerial is demonstrated using envelope correlation coefficient and radiation pattern. Additionally, it has been shown that simulated and measured results generally agree.

1. INTRODUCTION

When microwave communications that require extensive coverage are used, an antenna array is crucial. Multiple-band transceivers are required for modern communication. Using a mobile phone for voice communication, data transfer, GPS, Bluetooth, and Wi-Fi are just a few of the many functions it may perform. When one antenna is used for just one application, it takes up more space and performs worse. This can be fixed by using similar antennas, which also improves radiation performance overall. The difficulty is that each electrical gadget only has a little amount of space set aside for antennas. Electromagnetic interaction between the radiation patterns takes place when several antennas are put close together, and this phenomena is known as Mutual coupling (MC). Mutual coupling has a detrimental effect on MIMO antenna performance. Numerous antenna characteristics are changed, including impedance, received voltages, and radiation patterns. Under these conditions, it is anticipated that each antenna element in the array will operate independently and with considerable isolation. Therefore, it is essential to lessen MC's impact.

A MIMO antenna with strong port isolation and a decoupling network is built in [1]. Different decoupling networks are analyzed using MC in this case, and the best network is selected to lessen the impact. The monopoles in [2] are positioned back-to-back in an orthogonal and symmetrical arrangement. To reduce the mutual coupling, the monopoles are connected by a novel neutralization line (NL), which is made up of a parasitic rectangular ring and a straight strip line. The mutual coupling is substantially below $-15\,\text{dB}$ when NL is introduced. To lessen MC, F-shaped stubs are added to the ground plane in [3]. In [4], MC is reduced by shorting pins and employing slots. A resonator in the shape of a dollar is added between the two parts in [5] to lessen the impact of MC. Frequency selective surfaces are employed in [6] to reduce the MC between elements.

2. ANTENNA DESIGN AND GEOMETRY

The dimensions and geometry of the suggested antenna are shown in Figure 1. The suggested antenna has an FR-4 substrate and has ε_r and δ values of 4.4 and 0.02, respectively. The patch is taken in a circle with radius $R1$. After that, $R2$ is used to take another circular patch. A second $R3$-radius circular patch is taken and moved 3 millimeters to the left. It is taken away from $R2$. Table 1 displays the proposed antenna's optimal parameters.
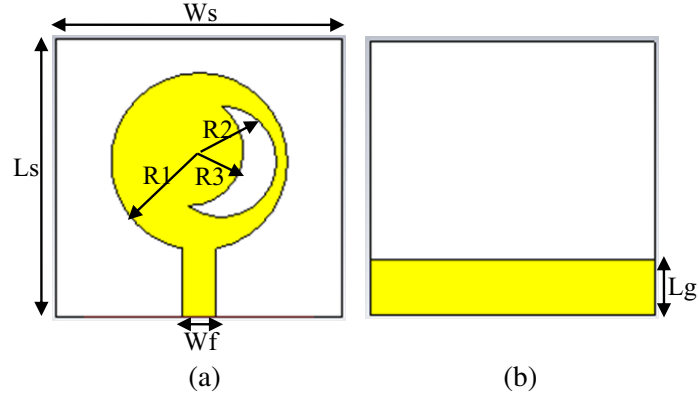
Figure 1. Proposed antenna. (a) Font view. (b) Back view.

Table 1. Optimized parameters and their dimensions.

Parameter	Ws	Ls	Wf	$R1$	$R2$	$R3$	Lg
Dimensions (mm)	26	25	3	8	5	5	5

2.1. Return Loss

Figure 2 depicts the suggested antenna's return loss curve (S_{11}). The frequency range of the suggested antenna is from 3.1 to 8.2 GHz. Return loss is seen to be -18 dB at 3.7 GHz and -24.2 dB at 7.2 GHz, respectively. The provided antenna is suitable for the use with UWB technology.
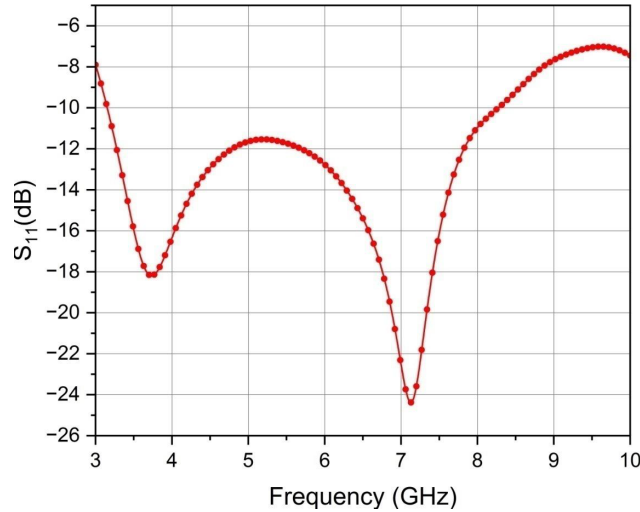
Figure 2. Return loss curve.

3. MIMO ANTENNA

The antenna in Figure 3 is also used by the 2×2 MIMO antenna. Two patch antennas are symmetrically arranged with respect to the origin. The two parts are 2 mm apart from edge to edge. A T-shaped stub is between the two antennas and has the dimensions Wt and Lt. The proposed MIMO antenna's optimal dimensions are shown in Table 2.
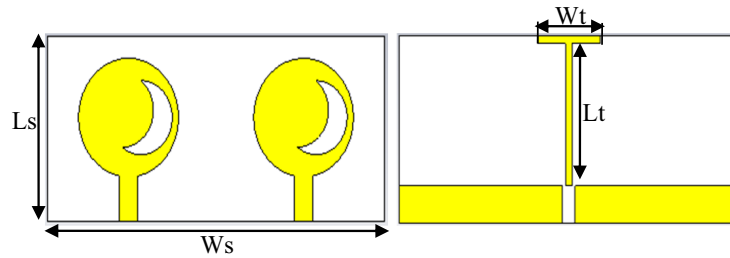
Figure 3. MIMO antenna.

Table 2. Optimized dimensions of the MIMO antenna.

Parameter	Ws	Ls	Wt	Lt
Dimensions (mm)	54	25	10	19

3.1. Return Loss

The suggested MIMO antenna's observed and modeled return loss curves are shown in Figure 4. It ranges between 3.1 and 8.2 GHz. Additionally, it has been noted that there is good agreement between simulated and measured outcomes.
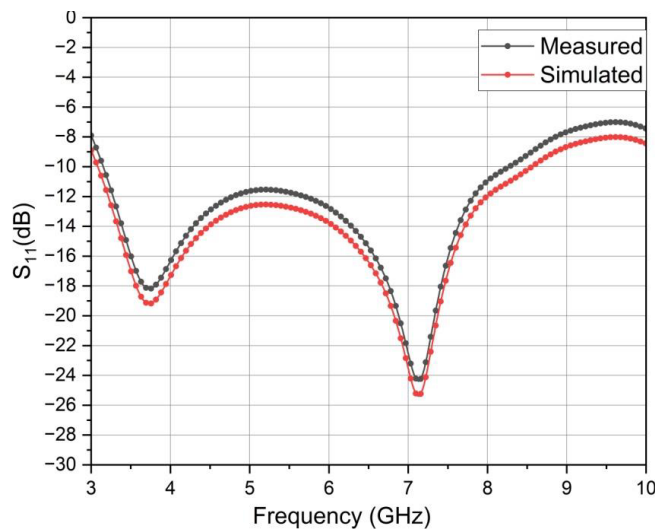

Figure 4. Simulated and measured S_{11}.

3.2. Mutual Coupling (MC)

The MIMO antenna's primary performance metric is mutual coupling. Mutual coupling is developed between two antennas when they are put in close proximity to one another. Since MC impairs the performance of the MIMO antenna, its reduction is necessary. Figure 5 displays the measured and simulated S_{21} for the suggested MIMO antenna. MC is seen to be lower than -15 dB in both bands.

The suggested MIMO antenna's MC is shown in Figure 6 both with and without the stub. Without a stub, it can be seen that the MC is high between 4.5 and 5.5 GHz in the marked area. The MC is lowered to below -15 dB over the entire band when the stub is inserted between the elements. It is observed that the MC is -4 dB lower with stub.
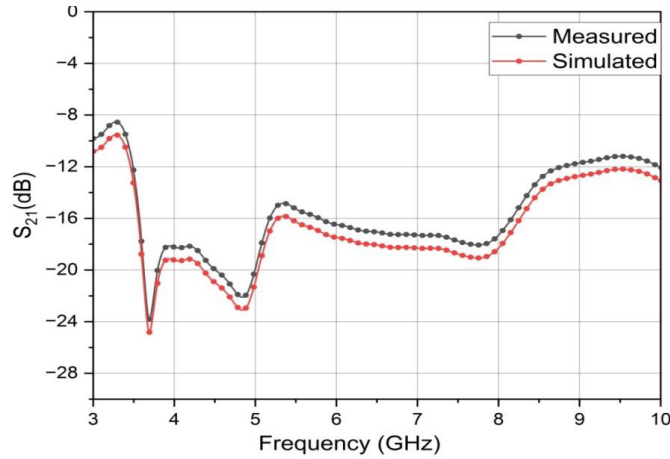
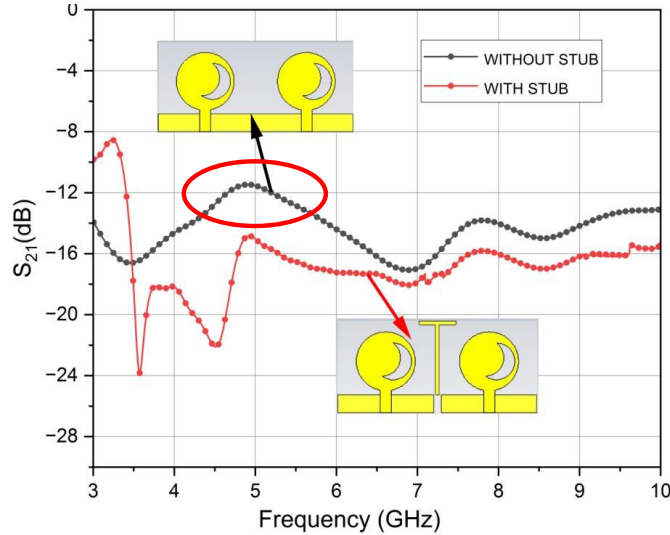**Figure 5.** Simulated and measured S_{21}.

Figure 6. S_{21} with and without stub.

Surface currents are recorded at 5.24 GHz, 6.39 GHz, and 8.68 GHz in order to gain physical insight into the mutual interaction between the constituents. As seen in Figure 7, the stub stops surface currents from moving from one element to another. Port 2 is terminated while port 1 is excited.
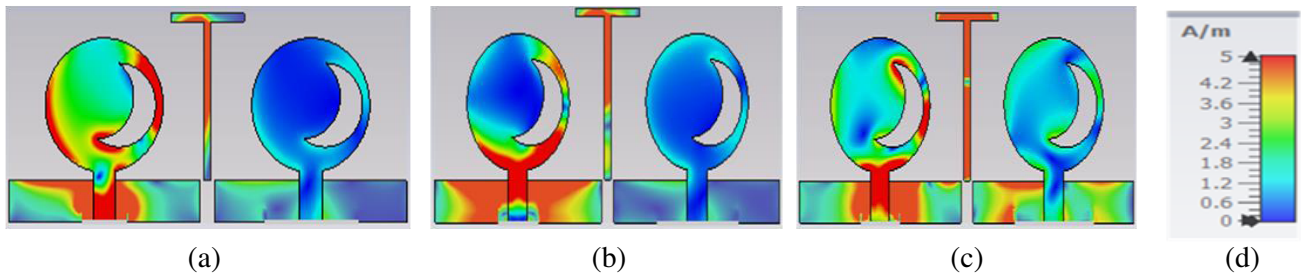
Figure 7. Surface current distribution (a) 5.24 GHz, (b) 6.39 GHz, (c) 8.68 GHz, (d) scale.
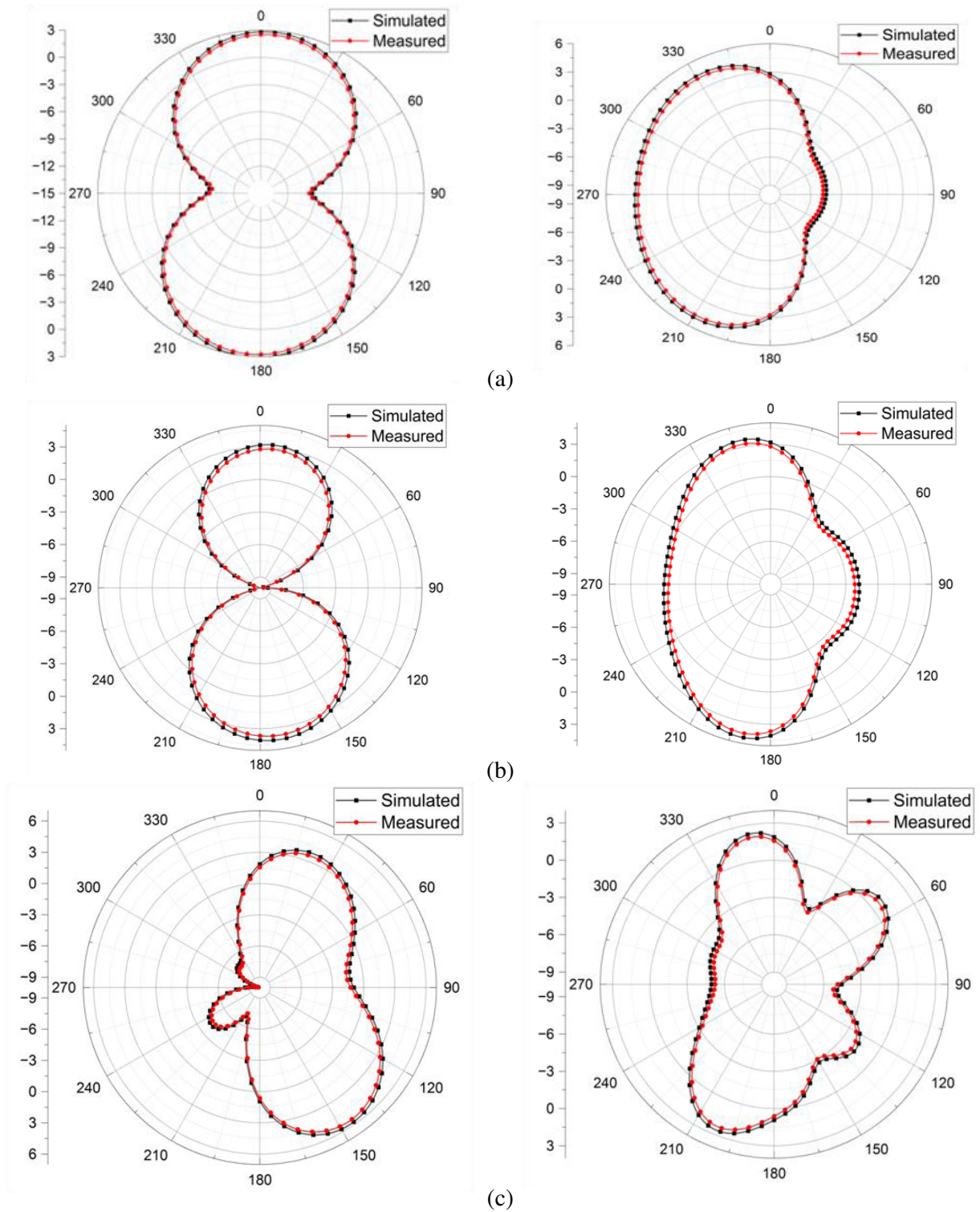
Figure 8. Simulated and measured radiation pattern in both *E*-plane and *H*-plane (a) 5.24 GHz, (b) 6.39 GHz, (c) 8.68 GHz.

Figure 8 shows the radiation pattern of the antenna in the *E*-plane and *H*-plane. The measured and simulated radiation patterns are comparable. Figure 8 depicts the constructed prototype of the suggested antenna.

Figure 9. Efficiency.

| (a) | (b) | (c) | (d) |
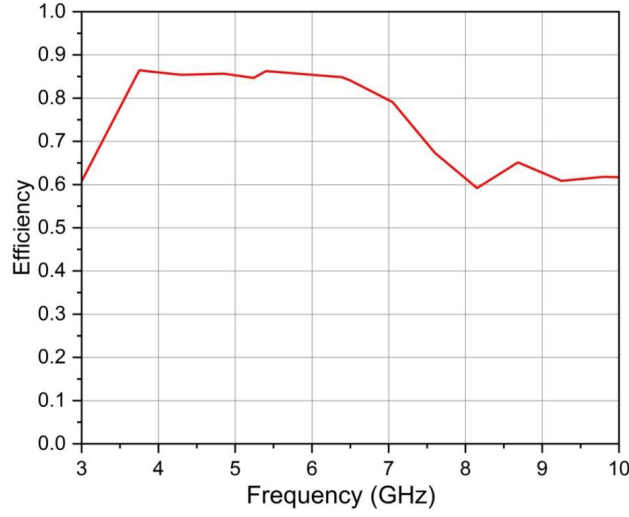
Figure 10. Fabricated antenna. (a) Front view, (b) back view, (c) vector network analyzer, (d) anechoic chamber.

The efficiency of the antenna is shown in Figure 9. Efficiency is above 80% over the entire operating band. The fabricated prototype and measurements using vector network analyzer and anechoic chamber are shown in Figure 10.

Diversity gain, multiplexing effectiveness, effective diversity gain, channel capacity loss, and envelope correlation coefficient can be used to evaluate MIMO performance.

Diversity Gain

To determine the diversity gain of the MIMO antenna, Equation (1) is applied. The diversity gain (DG) of the MIMO antenna is $9.98\,\text{dB}$ at $5.24\,\text{GHz}$, $6.39\,\text{GHz}$, and $8.68\,\text{GHz}$, respectively. Figure 11 displays a DG plot.

$$\text{DG} = 10\sqrt{1 - |\text{ECC}|^2} \tag{1}$$

Multiplexing Efficiency

The multiplexing efficiency and overall efficiency for a two element antenna are calculated using Equation (2).

$$|\rho_e|^2 = 1 - \frac{\eta_{mux}}{\eta_1 \eta_2} \tag{2}$$

The total efficiencies of antennas 1 and 2 are η_1 and η_2. η_{mux} is the multiplexing efficiency.
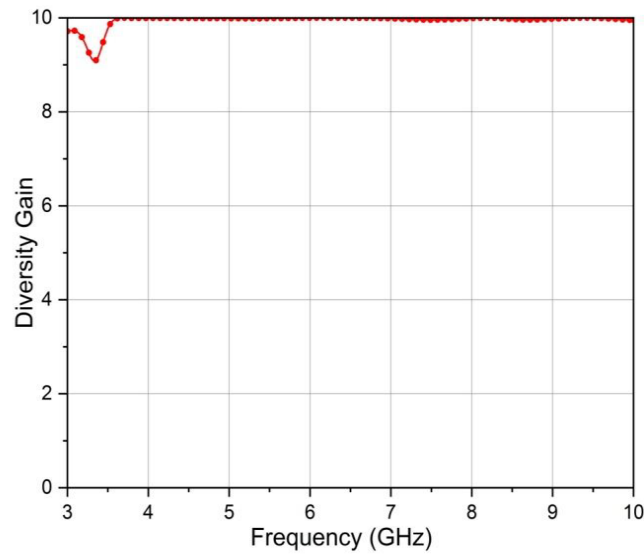
Figure 11. Diversity gain.

Effective Diversity Gain

The antenna efficiency, DG, and effective diversity gain (EDG) relation is shown in (3)

$$\text{EDG} = \text{DG} \times \eta_{ant} \tag{3}$$

Channel Capacity Loss (CCL)

One of the key performance indicators for MIMO antennas is channel capacity. CCL can be calculated using Equation (5).

$$C_{loss} = -\log_2 \det(\Psi^R) \tag{4}$$

$$\Psi^R = \begin{bmatrix} \rho_{11} & \rho_{12} \\ \rho_{21} & \rho_{22} \end{bmatrix}$$

$$\rho_e = \frac{|s_{11}^* s_{12} + s_{21}^* s_{22}|^2}{\left(1 - |s_{11}|^2 - |s_{21}|^2\right)\left(1 - |s_{22}|^2 - |s_{12}|^2\right)} \tag{5}$$

Figure 12. ECC.

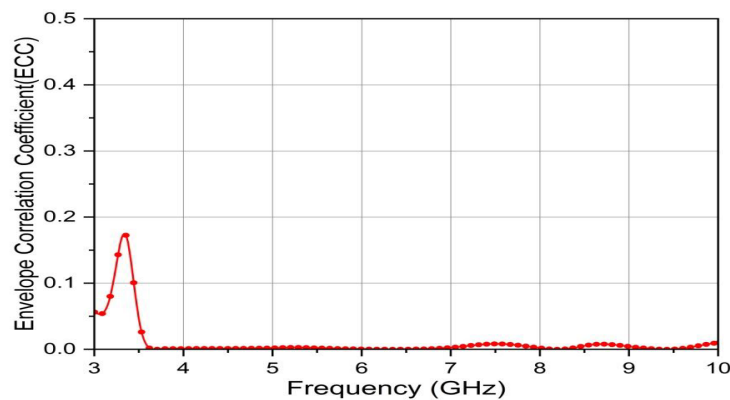With $\rho_{ii} = (1 - (|S_{ii}|^2 + |S_{ij}|^2))$ and $\rho_{ij} = -(S_{ii}^* S_{ij} + S_{ji}^* S_{jj})$ for $i, j = 1$ or 2.

Envelope Correlation Coefficient (ECC)

ECC is one of the most important factors to consider while evaluating the performance of a MIMO antenna. The association is always kept between the two sections at a minimum. ECC and diversity gain go hand in hand. The ECC decreases as DG increases. Equation (6) can be used to determine the envelope correlation coefficient curve for the proposed MIMO antenna from fields. The ECC is shown in Figure 12.

$$\rho_c = \frac{\int_0^{2\pi} \int_0^{\pi} XPRE_{\theta K}(\theta, \emptyset) E_{\theta l}^*(\theta, \emptyset) P_\theta(\theta, \emptyset) + E_{\emptyset k}(\theta, \emptyset) E_{\emptyset l}^*(\theta, \emptyset) P_\emptyset(\theta, \emptyset) \sin\theta d\theta d\emptyset}{\sqrt{\sigma_k^2 \sigma_l^2}} \tag{6}$$

The performances of the proposed antenna and those in literature are shown in Table 3.

Table 3. Comparison with literature.

Ref.	Size (mm^2)	Isolation (dB)	Bandwidth	ECC	Diversity gain	Efficiency %	Peak Gain (dB)
[7]	18×36	< -20	3–11	< 0.05	> 9.8	NA	4
[8]	40×20	-20	3.1–14	< 0.05	> 9.8	NA	0.4–5.7
[9]	50×35	< -25	3–11	< 0.004	NA	> 80	> 3
[10]	120×60	< -12.5	1–4.5	< 0.19	NA	NA	1.7–3.6
[11]	25×25	< -15	2.97–13.8	< 0.05	> 9.97	NA	NA
[12]	22×31	< -15	2.9–12	< 0.3	NA	NA	2.31
[13]	50×30	< -20	2.5–14.5	< 0.04	> 7.4	NA	0.3–4.3
[14]	31×43	< -15	3.9–8.1	NA	NA	NA	NA
[15]	50×40	< -15	2.5–11	< 0.01	NA	NA	2–8
Proposed	53×25	< -15	3.1–8.2	< 0.01	9.9	> 80	2–6

4. CONCLUSION

An innovative circular moon slot antenna is created and upgraded to 2×2 MIMO. The proposed MIMO antenna operates between 3.1 and 8.2 GHz. The impact of MC is reduced by a T-shaped stub construction. Results from measurements and simulation are quite similar. The suggested MIMO aerial's performance is further assessed in terms of ECC, DG, channel capacity loss, and radiation patterns. For UWB applications, the proposed MIMO antenna is the ideal option.

REFERENCES

1. Tangirala, G., S. Garikipati, D. M. K. Chaitanya, and V. K. Sharma, "High isolation four-port Wrench shaped compact UWB MIMO antenna for 3.1–10.6 GHz band," *Progress In Electromagnetics Research C*, Vol. 122, 67–82, 2022.
2. Kayabasi, A., A. Toktas, E. Yigit, and K. Sabanci, "Triangular quad-port multi-polarized UWB MIMO antenna with enhanced isolation using neutralization ring," *International Journal of Electronics and Communications*, Vol. 85, No. 3, 47–53, Feb. 2018.

3. Dalal, P. and S. K. Dhull, "Design of triple band-notched UWB MIMO/diversity antenna using triple bandgap EBG structure," *Progress In Electromagnetics Research C*, Vol. 113, 197–209, 2021.

4. Abu Sufian, Md., N. Hussain, H. Askari, S. G. Park, K. S. Shin, and N. Kim, "Isolation enhancement of a metasurface-based MIMO antenna using slots and shorting pins," *IEEE Access*, Vol. 9, 73533–73543, May 2021.

5. Mandal, S. and C. K. Ghosh, "Low mutual coupling of microstrip antenna array integrated with dollar shaped resonator," *Wireless Personal Communications*, Vol. 119, No. 1, 1–13, March 2021.

6. Thummaluru, S. R., R. Kumar, and R. K. Chaudhary, "Isolation enhancement and radar cross section reduction of MIMO antenna with frequency selective surface," *IEEE Transactions on Antennas and Propagation*, Vol. 66, No. 3, 1595–1600, March 2018.

7. Khan, M. I. and M. I. Khattak, "Designing and analyzing a modern MIMO-UWB antenna with a novel stub for stop band characteristics and reduced mutual coupling," *Microwave and Optical Technology Letters*, 1–6, May 2020.

8. Patra, P. K. and M. K. Das, "Modified ground with $50\,\Omega$ step fed WLAN notch 2×2 MIMO UWB antenna," *Int. J. RF Microw. Comput. Aided Eng.*, Vol. 30, No. 3, December 2019.

9. Wang, L., Z. Du, H. Yang, R. Ma, Y. Zhao, X. Cui, and X. Xi, "Compact UWB MIMO antenna with high isolation using Fence-type decoupling structure," *IEEE Antennas and Wireless Propagation Letters*, Vol. 18, No. 8, 1641–1645, July 2019.

10. Zhao, X., S. Riaz, and S. Geng, "A reconfigurable MIMO/UWB MIMO antenna for cognitive radio applications," *IEEE Access*, Vol. 7, 46739–46747, April 2019.

11. Singh, H. V. and S. Tripathi, "Compact UWB MIMO antenna with cross-shaped unconnected ground stub using characteristic mode analysis," *Microwave and Optical Technology Letters*, Vol. 61, 1–8, February 2019.

12. Li, W., Y. Hei, P. M. Grubb, X. Shi, and R. T. Chen, "Compact inkjet-printed flexible MIMO antenna for UWB applications," *IEEE Access*, Vol. 6, 50290–50298, August 2018.

13. Iqbal, A., O. A. Saraereh, A. W. Ahmad, and S. Bashir, "Mutual coupling reduction using F-shaped stubs in UWB-MIMO antenna," *IEEE Access*, Vol. 6, 2755–2759, December 2018.

14. Hakimi, S., S. K. Abdul Rahim, M. I. Sabran, A. N. Obadiah, and H. Mohamed, "Compact MIMO antenna for indoor UWB applications," *Microwave and Optical Technology Letters*, Vol. 58, No. 10, October 2016.

15. Lin, G.-S., C.-H. Sung, J.-L. Chen, L.-S. Chen, and M.-P. Houng, "Isolation improvement in UWB MIMO antenna system using carbon black film," *IEEE Antennas and Wireless Propagation Letters*, Vol. 16, 222–225, May 2016.